Proliferative arrest induces neuron differentiation and innate immune responses in control and Creutzfeldt-Jakob Disease agent infected rat septal neurons

Nathan Pagano, Gerard Aguilar Perez[1], Rolando Garcia-Milian[2] and Laura Manuelidis*

Yale University Medical School
333 Cedar Street, Room FMB11
New Haven CT 06510
203-785-4442

Key words: latent infection, epigenetic imprinting, cytokine storm, viral escape, proliferative transformation, prion

Running title: Neuron differentiation, innate immune transcripts and CJD infection

* To whom correspondence should be addressed: laura.manuelidis@yale.edu

[1] Current address Laboratory of Molecular Neuroscience, German Center for Neurodegenerative Diseases (DZNE), 10117 Berlin, Germany.
[2] Bioinformatics Support Hub, Yale Medical Library, Yale School of Medicine

ABSTRACT

Rat post-mitotic septal (SEP) neurons, engineered to conditionally proliferate at 33^0C, differentiate when arrested at 37.5^0C and can be maintained for weeks without cytotoxic effects. Nine independent cDNA libraries were made to follow arrest-induced neural differentiation and innate immune responses in normal (Nl) uninfected and CJ agent infected SEP cells. Proliferating Nl versus latently infected (CJ-) cells showed few RNA-seq differences. However arrest induced major changes. Normal cells displayed a plethora of anti-proliferative transcripts. Additionally, known neuron differentiation transcripts, e.g., Agtr2, Neuregulin-1, GDF6, SFRP4 and Prnp were upregulated. These Nl neurons also displayed many activated IFN innate immune genes, e.g., OAS1, RTP4, ISG20, GTB4, CD80 and cytokines, complement, and clusterin (CLU) that binds to misfolded proteins. In contrast, arrested highly infectious CJ+ cells (10 logs/gm) downregulated many replication controls. Furthermore, arrested CJ+ cells suppressed neuronal differentiation transcripts, including Prnp which is essential for CJ agent infection. CJ+ cells also enhanced IFN stimulated pathways, and analysis of the 342 CJ+ unique transcripts revealed additional innate immune and anti-viral-linked transcripts, e.g., Il17, ISG15, and RSAD2 (viperin). These data show: 1) innate immune transcripts are produced by normal neurons during differentiation; 2) CJ infection can enhance and expand anti-viral responses; 3) latent CJ infection epigenetically imprints many proliferative pathways to thwart complete arrest. CJ+ brain microglia, white blood cells and intestinal myeloid cells with shared transcripts may be stimulated to educe latent CJD infections that can be clinically silent for >30 years.

INTRODUCTION

There are relatively few papers analyzing cDNA libraries of normal differentiating neurons in culture as they transition from a proliferative to an arrested G1 state. Post-mitotic neuron differentiation in animals takes place over many days with differentiation times determined by species and neuronal cell type [1]. Studies of neuron differentiation in brain are complicated by cellular and humoral complexity. Neuroectodermal cells (as astrocytes), along with vascular endothelium, microglia, and blood borne factors (serum molecules and hormones) can have multiple effects on core neuronal differentiation and cell fate programs. Cultured rat post-mitotic septal (SEP) neurons, immortalized with a temperature sensitive (ts) SV40 construct, provides a powerful model for studies of neural differentiation over a 3-4 week period without these complications [2, 3]. We are not aware of any reports of post-mitotic neurons where differentiation can be reversibly turned on and off for weeks, a feature that can be particularly informative for understanding latent viral infections.

SEP cells proliferate at 33°C and can be physiologically arrested at 37 ^{0}C in 2 % serum. Arrested cells stop synthesizing DNA by 4-6 days post-arrest, as assessed by BrdU incorporation in nuclei, and these cells can be maintained in an arrested state by refeeding every 2 days for >75 days without reverting to a proliferative state [4]. During this time, cell-to-cell contacts and neural markers increase along with host prion protein (PrP), assayed on western blots, and host gene transcripts (Prnp) assayed by RT/qPCR [4, 5]. PrP is a neural differentiation marker that increases during synaptogenesis and PrP localizes to membranes by electron microscopy [6]. It is also a required host factor for infection in CJD and other Transmissible Spongiform Encephalopathies (TSEs) [7], and its misfolded or amyloid form is a marker of disease. Previously, RT/qPCR studies of normal SEP cells were limited to a few chosen molecular markers and did not address more global changes, some of which may be unsuspected. Large scale cDNA libraries were made here to reveal transcripts and networked pathways induced during arrest. Because previous RT/qPCR studies of normal SEP neurons showed arrest induced upregulation of β-interferon (β-IFN), a classical innate immune

response [4], cDNA libraries were interrogated to confirm and expand additional immune changes that might accrue in these normal samples during neuronal differentiation.

Parallel studies of normal rat SEP cells infected with the rat passaged human FU-CJD agent [5, 8] provided an intriguing comparison because arrested SEP cells produced persistent high titers of the infectious agent (9.7 logs/gm for 120 days) as well as pathologic PrP amyloid without visible cytotoxic or neurodegenerative stigmata seen in CJD brain. Misfolded PrP amyloid appears late in disease brain, after agent has silently replicated to high levels, e.g.7-8 logs/gm [9]. When highly infectious (CJ+) SEP cells are allowed to proliferate at 33^0C they rapidly lose 4 logs of infectivity along with PrP amyloid [5]. To determine if these proliferating SEP cells with no detectable infectivity (CJ-) were latently infected, they were re-arrested. Again they produced very high levels of infectious agent (10 logs/gm), proving latent, phenotypically silent infection in the CJ- proliferating cells. These re-arrested cells also displayed some PrP amyloid, and they upregulated β–IFN transcripts by 60 fold [4]. These CJ- and CJ+ cells were used to make libraries here to identify additional major cellular modifications that might accrue during latent CJD infections. Latent infections can be very extended in people. For example, cannibalism associated kuru in New Guinea can take >10 years to produce disease after peripheral exposure [10], and CJD contaminated growth hormone infections can remain latent for at least 30 years [4]. Since not all people exposed to kuru and CJD by an oral or cutaneous route develop disease, a remaining subset of the population exposed to TSEs may continue to harbor silent infections that have not been detected. Thus it is pertinent to point out key biological features TSEs and latent infection, a state that is largely forgotten in studies focusing on PrP amyloid.

Latency in CJD and other Transmissible Spongiform Encephalopathies (TSEs) is informed by experimental animal studies. Endemic sheep scrapie, a neurodegenerative disease recognized for over 500 years, human sporadic Creutzfeldt-Jakob Disease (sCJD), and epidemic “mad cow” disease (BSE) belong to a group of Transmissible spongiform encephalopathies (TSEs) [11]. Fundamental

infectious and pathologic features of TSEs were first demonstrated in 1936 by serial passage of sheep scrapie brain [11]; Wilson showed the scrapie "virus" efficiently passed through 0.41μ filters, and caused disease via various inoculation routes, e.g., intracerebral, intravenous, cutaneous [12]. Successful transmission of the scrapie virus to rodents in the 1960s, critical for pathogenesis studies, showed the incubation time to disease after inoculation (latency) was dependent on dose, route and species susceptibility, and lymphoid tissue infections (a latent reservoir) preceded brain infections by 10 weeks [13]. Transmission of sCJD to small animals in the 1970s added other medically relevant findings such as white blood cell infection, and lack of maternal transmission [14]. As in scrapie, different CJD agent strains were identified by latency and the distribution and severity of brain lesions [11, 15]. In normal mice the sCJD agent is slow and produces minimal lesions while the Asiatic FU-CJD strain replicates rapidly and produces widespread destructive lesions. Despite this difference in virulence both agents show indistinguishable PrP amyloid characteristics. In general, PrP amyloid is not strain-specific [16] but cell-type specific [17]. Nevertheless, powerful virulence differences of sCJD and FU-CJD were additionally demonstrated by a classical viral vaccination strategy. Inoculation of the human slow sCJD agent-stain prevented superinfection by FU-CJD agent-strain in mice, and also in cell cultures; in the latter additional scrapie agent-strains were compared were also distinguished [16, 18, 19]. These strain findings are of relevance because in principle, latent infection could underlie resistance to infection by more virulent neurodegenerative strains.

Since the differentiation of various types of neurons is exquisitely connected to specific sequential times of development, we compared representative early and later post-arrest days in parallel studies of uninfected and CJD infected SEP cells. To ensure the high reproducibility of major transcript and pathway changes, different independent SEP cell passage groups at multiple days after arrest were compared using the most relevant and representative time points based on previous RT/qPCR, protein and shared cellular marker studies [3, 4].

MATERIAL AND METHODS

Cell Culture characterizations: All experiments and cultures used to make cDNA libraries were previously described in detail [4]. Briefly, low passage post-mitotic rat Septal (SEP) neurons, immortalized with a temperature sensitive ts-SV40 T antigen (subclone e422, [1]), were passaged every 4 days at 1:4 in a proliferating state at 33ºC in 10% serum-DMEM. To induce and maintain arrest, cells were cultured in 2% serum-DMEM at 37.5ºC and refed every 2 days without splitting. Normal arrested cells became 95% stationary by day 2, shown by cessation of BrdU incorporation into DNA and loss of SV40 T antigen protein (Tag) e.g., [2]. With arrest, prion protein (PrP) progressively increases to 15-20x the normal uninfected level in SEP cells from passages 7, 17 and 25 [4], and these arrested and parallel controls were used here for cDNA libraries and analyses. Briefly, thawed untreated normal cells from these different passages were either allowed to proliferate, or maintained in an arrested state for the indicated days of each passage set. Independent groups of parallel proliferating and arrested cells from the same day were compared. Proliferating and arrested cells from these 3 independent passages showed comparable patterns of PrP, SV40 Tag and β-IFN changes. Fig. 1A summarizes these proliferating control uninfected cells in light green (Prol/Nl) with their parallel arrested cells sampled on the same day in darker green (Arst/Nl).

Fig. 1A also shows two CJD groups with control proliferating cells (Prol/CJ-) in light orange, and their parallel re-arrested counterparts in dark orange (Arst/CJ+). More specifically, proliferating SEP cells that had been infected with FU-CJD rat brain homogenate [8] that were arrested for 75 days attained a high titer of 5 tissue culture infectious doses per cell (TCID), equivalent to 5E9 infectious particles/gm where 1gm of brain contains 10^9 cells in standardized assays as described [5, 20, 21]. These high infectivity cells were frozen at passage 17 (p17). They were then thawed and allowed to proliferate for 3 additional passages. Even with 1 passage of release from arresting conditions, the high CJD infectivity of 5 TCID/cell ($5x10^9$/gm) was substantially lost and reduced to 2 TCID/1,000 cells ($2x10^6$/gm), i.e., a loss of >3 logs [5]. Thus, proliferating SEP cells are designated Prol/CJ- to

indicate they lost all detectable infectivity after further passaging these samples [4]. These CJ-controls were pertinent because the effects of previous high FU-CJD infection might alter standard normal SEP cell characteristics. In the current experiments, at passage 3 after thawing, proliferating FU-CJD SEP cells were re-arrested and maintained in parallel with their CJ- controls. By 6 days and 34 days post-arrest their infectivity increased to 2 TCID/cell (9.3 logs/gm) and 10 TCID per cell (10 logs/gm) respectively in standard GT1 indicator cell assays as depicted [4]. TCID infectivity assays correlate well with LD_{50} animal agent titrations, and re-inoculation of infected cells also reproduce their strain-specific characteristics in mice. These high infectivity FU-CJD SEP cells are designated Arst/CJ+. Selection of passage and sample days for both normal and CJD groups here were based on protein and RT/qPCR cDNA analyses as graphically detailed [4] for elevated β-interferon, Prnp and absent Tag RNAs in addition to relevant protein changes including protease resistant PrP amyloid.

RNA sequencing: Brett Robb and staff at New England Biolabs generously constructed the cDNA libraries and performed the RNA sequencing for the above samples. Between 72-92 ng of RNA per sample was subjected to rRNA depletion via the NEBNext® rRNA Depletion Kit v2 (Human/Mouse/Rat; NEB #E7400) using the manufacturer's protocol except that a Monarch® RNA Cleanup Kit (10 µg; NEB# T2030) was used to purify the rRNA-depleted RNA instead of magnetic beads. The rRNA-depleted RNA was converted [15] into Illumina-compatible DNA libraries via the NEBNext® Ultra™ II Directional RNA Library Prep with Sample Purification Beads kit (NEB# E7765) using the manufacturer's protocol for use with rRNA-depleted RNA and NEBNext® Multiplex Oligos for Illumina® (NEB# E6448). Samples were pooled and sequenced 2x150 nt paired-end on an Illumina® Novaseq 6000 instrument.

RNA bioinformatic analysis: Partek™ Flow™ software (version 11) bulk RNA-seq pipeline was used for data analysis. In summary, trimmed reads were aligned to the Rnor_6.0 (rn6) genome reference using STAR [22] (version 2.7.8), and subsequently Partek E/M algorithm [23] was used to count reads mapping to the genes from Ensembl release 95. We applied the DESeq2 normalization

method and top 1000 genes by variance were analyzed for PCA. Heatmaps show row-normalized relative gene expression z-scores across columns. Qlucore Omics Explorer (Qlucore, Lund, Sweden), a dynamic, interactive visualization-guided bioinformatics program with a built-in statistical platform was used for data visualization. Differential expression was performed using the DESeq2 [24] method. The cutoff value to select differentially expressed genes was Log2ratio ≥ |0.5|, FDR $p<0.05$ [25]. A copy of the dataset was stored in the National Center for Biotechnology Information, Gene Expression Omnibus database: GSE272571

Functional analysis: Overrepresented pathways, biological functions, upstream regulators, and biological networks were identified using Ingenuity Pathway Analysis (QIAGEN Redwood City, CA) knowledgebase and g:Profiler [26]. For this, differentially expressed gene identifiers are mapped and analyzed using a one-tailed Fisher Exact Test, (FDR $p< 0.05$). In addition, Gene Set Enrichment Analysis (GSEA Mac App Broad Institute Inc.) [27] was performed using DESeq2-normalized counts with gene set permutation and otherwise default settings. By using the Rat_Gene_Symbol_Remapping_Human_Orthologs-MSigDB v7.2 chip, gene counts were tested against the human hallmark (H), canonical pathways (C2), gene ontology (C5), and immunologic signature (C7) gene sets (version 7.5.2). Gene sets with false discovery rates (FDR) $p< 0.25$ were considered enriched as suggested by GSEA developers. The overlap and connections between the resulting different gene sets were produced by the Enrichment Map Plugin (http://baderlab.org/Software/EnrichmentMap) for Cytoscape 3.8 [19], considering a value of FDR $p< 0.05$. The nodes were joined if the overlap coefficient was ≥ 0.375.

RESULTS

Hierarchical clustering of 9 independent cDNA libraries. For comparative analyses, 9 independent SEP cell cDNA libraries were made from the uninfected and infected cell RNA extracts in experiments using different SEP cell passages for arrest. These libraries were chosen based on the day of the initial increase in Prnp (by RT/qPCR and PrP amyloid western blots), and β-IFN

transcripts. Both transcripts rose steeply by 6-8 days after arrest. Arrested cell RNAs and their parallel proliferating controls were assayed sequentially every 4-6 days for up to 35 days post-arrest [4] at the selected passages and days indicated in Fig 1A. Representative libraries, colored green for uninfected, and red for CJ agent infected, fell into distinct proliferating (lighter shades) and arrested (darker shaded) groups (Fig. 1A). The proliferating uninfected normal (Nl) control sets, sampled at 2 different passages (p7 and p25), fell into group 1, and are designated Prol/Nl. These Nl proliferating transcripts were closely related to CJ- proliferating transcripts in group 2 (p17 and p20). Remarkably, despite their prior infection, these CJ- proliferating cells revealed only 19 differentially expressed transcripts (8 up & 11 down regulated). In contrast, comparison of both arrested groups 3 and 4 (Arst/Nl and Arst/CJ+) contained 379 differentially expressed genes. Fig. 1B shows the divergence of the uninfected Nl groups 1 and 3 by principal component analysis along with a clustering of reproducible Prol/Nl vs Arst/Nl differences in independent experimental samples (group 2 proliferating vs group 3 arrested). Notably, the Arst/Nl vs Prol/Nl sets contain more downregulated (blue) than upregulated (yellow) genes in each of the two p25 Arst/Nl RNAs samples at different days in culture (6 and 14 days). An independent second repeat experiment from p7 also has a highly similar cDNA profile as shown in the Fig. 1B. As in the Nl controls, Arst/CJ+ cells again segregate in a distinct group from Prol/CJ- cells . However, as shown in 1C the CJ differential analysis resulted in only 112 differences as compared to 379 in uninfected SEP cells. Moreover, whereas downregulated genes dominated in the Arst/Nl cells, 60% of the transcripts in CJ+ arrested cells were upregulated.

Comparison of proliferating uninfected and CJ- cDNAs. While there were only 19 differences between proliferating Nl and CJ- cell sets, several of these suggested stable transcriptional changes caused by prior infection. The Prol/CJ- transcripts reproducibly contained upregulated acute phase protein LPB (up 7.2-fold) involved in innate immunity, and inflammation associated complement C1s (up 3.5-fold in the Prol/CJ- set). Mt1m was also upregulated 5.2-fold, and this zinc binding protein is high in several brain regions and localized to the perinuclear region where PrP

amyloid fibrils aggregate in infected cells [6]. Six downregulated genes were also notable, including Apoe, down 5.8 fold, Adamts8 metallopeptidase, down 5.8 fold, and Cavin4 (down 9.1 fold) that encodes a Golgi and plasma membrane caveolar protein in synaptic vesicles, and possibly linked to vacuolar "spongiform" dendritic and synaptic changes in TSEs [28]. Tspan7, a transmembrane glycoprotein functionally involved in many different viral infections [29] was downregulated 10 fold, and neuron development genes Tenm3 and Dpysl3 were down 19.4 fold and 26.8 fold respectively in Prol/CJ- vs Prol/Nl cells. To best appreciate the diversity and extent of specific changes in the 4 major groups, differential changes between uninfected SEP cells (Arst/Nl and Prol/Nl) are analyzed first, and then the CJ infected samples compared.

Arrest produces many transcriptional changes in uninfected SEP cells: To assess reproducibility of changes we compared the 25 most downregulated transcripts in each of the 3 arrested Nl cDNA sets. All these genes were present in at least 2 of these 3 independent samples regardless of function (Supplement Table S1). The most downregulated transcripts (5 to 53-fold lower) are suppressed during DNA replication and cell cycle progression, including cell cycle checkpoints, histone synthesis (with 4 different histones lower by 6.5 to 28x) and spindle microtubule formation. A total of 18/25 downregulated genes localized to the nucleus. The longest Nl arrest sample (p25 at 14 days) showed all these genes were downregulated whereas the shorter 6 and 7 day arrested samples displayed some variants (6 and 8 respectively) including two histone transcript clusters that were absent, as they normally would be during the S phase of growth. Other minor fold variations in the top 25 transcripts, such as Cenpf, are also consistent with an initial lack of synchrony of G1, S and the shorter mitotic cell cycle phases; this was supported by the increased time needed to achieve a complete and stable synchronous arrest in G1. The total differential RNAseq data further emphasizes multiple processes involved in SEP neuronal arrest were orchestrated precisely and sequentially, as during transitions though DNA replication and mitosis, and all were educed by physiological arrest. Upregulated top genes in Arst/Nl were uniformly changed in all three

independent samples (Table 1). Three nuclear anti-proliferative upregulated transcripts are seen with diverse other transcripts localized

			P7, 7d		P25, 6d		P25, 14d		
#	Rat Symbol	Entrez Gene Name	FDR(p)	Log2Ratio	FDR(p)	Log2Ratio	FDR(p)	Log2Ratio	Location
1	Rbp2	retinol binding protein 2	3.67E-02	7.855	9.75E-03	10.813	4.46E-03	11.341	Cytoplasm
2	Sulf2	sulfatase 2	1.61E-04	3.498	2.60E-11	5.515	5.20E-12	5.668	Plasma Membrane
3	Clec2d2	C-type lectin domain family 2, member D	1.42E-05	5.549	2.54E-04	5.329	1.54E-04	5.445	Plasma Membrane
4	Itm2a	integral membrane protein 2A	2.04E-03	3.919	9.20E-06	5.03	1.07E-06	5.344	Plasma Membrane
5	Cfh	complement factor H	3.35E-02	2.701	2.61E-06	5.007	1.15E-07	5.506	Extracellular Space
6	Mmp13	matrix metallopeptidase 13	6.42E-16	6.419	1.70E-07	4.827	4.76E-08	5.017	Extracellular Space
7	Sfrp4	secreted frizzled related protein 4	1.17E-02	3.079	2.48E-04	4.092	6.43E-05	4.329	Plasma Membrane
8	Ephx1	epoxide hydrolase 1	2.04E-03	3.141	2.16E-05	3.969	1.14E-05	4.031	Cytoplasm
9	Ccdc80	coiled-coil domain containing 80	4.02E-02	2.089	1.70E-07	3.899	6.28E-07	3.737	Nucleus
10	Cdkn1a	cyclin dependent kinase inhibitor 1A	4.55E-03	2.597	3.82E-03	3.757	6.71E-03	3.611	Nucleus
11	Svep1	sushi, von Willebrand factor type A, EGF & pentra	9.95E-05	3.588	6.45E-05	3.618	9.41E-07	4.196	Cytoplasm
12	Clu	clusterin	1.12E-06	4.097	7.05E-07	3.585	1.86E-06	4.028	Cytoplasm
13	Abca1	ATP binding cassette subfamily A member 1	4.92E-04	3.37	2.93E-04	3.477	1.54E-04	3.579	Plasma Membrane
14	Mmp2	matrix metallopeptidase 2	1.19E-04	3.108	1.32E-05	3.419	6.40E-06	3.473	Extracellular Space
15	Plk2	polo like kinase 2	3.35E-02	2.759	8.51E-03	3.177	1.18E-02	3.05	Nucleus
16	Tnn	tenascin N	3.83E-04	2.852	1.70E-03	2.964	2.53E-03	2.867	Plasma Membrane
17	C1s	complement C1s	3.76E-04	3.22	4.52E-03	2.891	5.72E-03	2.845	Extracellular Space
18	Edil3	EGF like repeats and discoidin domains 3	3.29E-02	2.492	1.19E-02	2.78	1.88E-03	3.127	Extracellular Space

Table 1: consistent upregulation of 18 genes (Log2Ratio) in 3 independent Arst/Nl samples.

to the plasma membrane or extracellular space, at least in vivo (C1s). Ingenuity pathway analysis showed a very complex network of many replication-related genes and further demonstrated the extent of anti-proliferative upregulated genes in the entire data set. The entire Arst/Nl data can't be graphed with any visual clarity due to all the participating pathways, so an example (from passage 7, day 7 transcripts) is shown in Fig. 2.

Neural differentiation genes are upregulated with arrest . 18 highly upregulated transcripts were consistently represented in all three Arst/Nl samples at different times post-arrest (Table I). These upregulated cDNAs were more diversified functionally than those that were downregulated. They included the 1,023-fold upregulated retinol binding protein 2 (Rbp2) active in neural differentiation, a calcium channel (Clec2d2) involved in neuronal networks, and Sushi (Svep1) a transcript which encodes a multidomain adhesion protein involved in epidermal differentiation [30] but not yet evaluated in neuron differentiation. The entire non-selected set of genes highlighted additional neuron differentiation characteristics. Fig. 3 shows the 4 transcripts with the strongest neuronal effects (darkest red) and 11 other major transcripts activating differentiation of neurons

listed (lighter red). Of these, neuregulin 1 (NRG1) and angiotensin receptor 2 (AGTR) promote neurogenesis but have other non-neural actions. However, neuregulin HES6* (Fig. 3), a helix-loop-helix transcription repressor that promotes neuron differentiation and inhibits astrocyte development [31], is largely limited to brain and endocrine tissue expression. GDF6, another strong contributor to hippocampal neurodifferentiation is also linked to wnt-neural fate (Fig. 4, circle 6). This The prion protein gene (Prnp) was also elevated in Arst/Nl cells, in accord with Prnp RNA upregulation previously identified by direct RT/qPCR analyses. Finally, the Nl neurodifferentiation transcripts appeared to be independent from the upregulated IFNs and inflammatory transcripts. Rather, neuron differentiation here was induced by the anti-proliferative transcripts.

Arrest induces IFN stimulated and innate immunity responses in uninfected cells: Table 1 also shows strongly upregulated immune-associated complement factors Cfh (21-fold) and C1s (8-fold). In these monotypic neural cultures, there is no extrinsic source of complement RNAs so they must be endogenously produced. In addition, the glycoprotein clusterin, a chaperone and complement regulating factor was significantly elevated. Its elevation in Nl arrested cells shows it is not linked to infection. The upregulation of Clu (clusterin) [32] and complement factors was unexpected. However, although not linked to neuron differentiation in the database, complement has been shown to be produced by neuronal cells in culture [33]. Analysis of the entire set of upregulated Nl arrest vs proliferating transcripts further expands and highlights distinct transcript sets according to function (term). Downregulated transcripts were again dominated by anti-proliferative functions as shown in Supplement Fig. S2. Additionally a small set of RNA processing features, including mRNA splicing, are known to be involved in selecting neuron specific RNA isoforms during neuron differentiation. Upregulated transcripts fell into a large “anti-viral defense” set that contained innate immune functions (Fig. 4, circle 1). Neuronal-linked differentiation transcripts form two separate sets: A) with complement activation and neurite processing/synaptic elaboration (circle 3) and B) Wnt-Neural fate pathways (circle 6). Upregulated anti-proliferative pathways and less specific signaling activities are

also seen. Together Figs. 3 and 4 indicate innate immune transcripts separately contribute to neuron differentiation in uninfected SEP cells rather than any anti-viral response.

Ingenuity pathway analyses expanded number of innate immune transcripts linked neuron differentiation. Many of these highly upregulated anti-viral transcripts are induced by IFNs, especially IFNγ as shown in Supplement Fig. S3 which shows strong upregulated viral responsive transcripts including TLR3, TRIM14, RTP4, RSAD2, ISG20, OAS1, GBP4, CD80 and MMP13 as well as multiple weaker IFN-induced transcripts. The extent of this group further verifies the upregulation of β-IFN found previously by direct RT/qPCR [4]. It also underscores many additional IFN stimulated transcripts in Arst/Nl cells including IFN-γ, IFN receptor (IFNar), Isg20 and others including upregulated Ifr7 (see complete deposited dataset). Gene Set Enrichment analysis in Supplement Fig. S4 further solidified the strong upregulation of IFNA, IFN-B1 and STAT 1 targets, with corresponding downregulation of EGFR and G2-M cell cycle signaling. DNA methylation was also downregulated during arrest, consistent with enhanced transcriptional activity of the neural differentiation transcripts identified, rather than a detrimental cell stress or toxic change.

In sum, physiological arrest induced a network of robust IFN responses unrelated to infection that are typically linked to innate immunity. The arrested cells displayed no cytopathic or toxic effects and remained in an arrested state for many days. The interferon network revealed above appears to be integral to the differentiation program at least for some neuronal types, and complement, typically associated with innate immune and anti-viral responses, appears to participate positively in this process. By comparison, CJ infected cells that could not be superficially distinguished from uninfected cells in the proliferative state, after arrest revealed major global transcript differences affecting proliferative pathways, neural differentiation and several innate immune responses.

Arrested CJ+ infected versus proliferating CJ- transcripts: As shown in Fig 1C prior CJ infection dramatically changed the latently infected CJ- cell phenotype as evidenced by the reduced scale and range of transcripts elicited by arrest. Most differences in this comparison showed up as a

failure to inhibit DNA replication and cell cycle checkpoint pathways in arrested CJ+ cells. For example, 23 different histone transcripts were upregulated in both sets of CJ+ cells (at 6 and 34 days that contained 9.3 and 10 logs/gm respectively). This coincided with limited ongoing cell division. In contrast, none of these histones were down regulated in Arst/Nl samples (Supplement Table S1). The significant downregulation of the ABRA signaling pathway that conveys external signals, including serum signals, further shows escape from the low serum environment that induced complete arrest in uninfected cells. Either CJ- cells were imprinted by previous infection, priming them to escape or resist arrest and/or recrudescence of high infectious agent titers during arrest-activated proliferation pathways. Upregulated proliferative transcripts in CJ+ cells were expected because CJD+ cells had to be split 16-18 days after arrest whereas uninfected cells remained in a non-proliferative state for 27 days [4]. The extent and number of proliferative activated transcripts identified here were very large and not anticipated.

Minimized neuronal differentiation in CJ+ cells. Combinatorial comparisons underscored more granular differences including a diminished activation of neuron differentiation transcripts in CJ+ cells. Supplement Fig. S5 compares CJ+ versus Prol/Nl and Prol/CJ- cells and segregates common and unique cDNAs in uninfected and CJ+ arrested samples. A reduced number of strong neuronal differentiation transcripts is apparent in Arst/CJ+ vs Prol/CJ- sets. This underscores an imprinted or permanent changes in latently infected CJ- cells that limits neuron specific development. For example, Wnt (Wnt5a) signaling is upregulated in Arst/Nl cells (Fig. 4) and this transcript positively regulates neuron maturation, synaptogenesis and axonal and dendritic outgrowth. In contrast, the opposite was found in CJ+ samples that showed strong negative regulation of canonical Wnt signaling. Moreover, Cavin4, an important component of synaptic caveolae was upregulated in Nl cells but downregulated in all CJ cells, including proliferating CJ- cells. This is consistent with an imprinted memory that permanently limits synaptic elaboration in latently infected cells.

Combinations of different sets of uninfected and infected samples further expanded major differences in CJ+ and Nl cells as seen in Fig. 6. Highest z scores in the Arst/Nl vs Prol/Nl comparison shows strong downregulated (blue) pathways. In contrast, the highest z scores in Arst/CJ+ vs Arst/Nl are upregulated genes that enhance DNA synthesis and cell division, or that have unrelated functional changes. Moreover, five of these same pathways (dotted in red) show opposite regulation between the two sets (Fig. 8, 2 top rows). These examples indicate the depth and range of escape from anti-proliferating signal in CJ+ cells. To complete the comparisons for CJ+ changes, the bottom two sets compare Arst/CJ+ to itself (Prol/CJ-) and to Prol/Nl. These comparisons highlight additional major differences between Nl and CJ+ samples. Notably, the highest CJ+ scores included hyperchemokinemia, caused by viral and other pathogens, cytokine storm signaling transcripts, and proinflammatory Il17 upregulation that promotes and exacerbates viral induced effects. These are not present in the comparable Nl control set with lower upregulated z-scores (Fig. 8, top left). Degradation of extracellular matrix and Matrix Metalloproteinases are also high in this CJ+ set but absent in the Nl set. These CJ+ differences indicate their strong link to high titers of agent rather than to IFN related changes common to both Nl and CJ+ arrested cells.

22 transcripts activate anti-viral activity in CJ+ cells. Ingenuity pathways yielded additional immune and anti-viral distinctions between Arst/CJ+ and Prol/Nl sets. These included both up (red) and down (green) regulated RNAs as indicated by their blue lines. Major strong regulators are listed. The strongest Mx1* gene, induced by IFNs, antagonizes the replication process of several different RNA and DNA viruses. Antiviral HERC6, ISG15, Itgb3 and IFIT 3 were all identified as strong activators in CJ+ cells as shown in Fig. 7. This anti-viral response also revealed a strong interactive network with the IFNs upregulated in the CJ+ dataset and is shown with cellular sites of action (Supplement Fig. S6). In CJ+ cells the IFNs are not extracellular in origin but made by the cell since no other cells are present to produce activating cDNAs. This data again substantiates RT/qPCR direct

experimental results in CJ+ cells: IFNs were far higher than in uninfected cells, indicating IFN enhanced transcripts were activated by the recrudescence of productive infection.

Stronger innate immune and anti-viral patterns in CJ+ vs Nl cells. IPA graphic analysis of signal strength in comparative Nl and CJ+ sets further solidified the above findings as shown in Fig. 8. Panel A shows 11 of 16 upstream regulators produced in CJ+ cells (red) are not present in Arst/Nl cells. Panel B shows selected canonical pathways with pathogen induced hyperchemokinemia, cytokine storm, matrix metalloproteinases and Il17 in CJ+ samples. These were not upregulated in Arst/Nl cells.

Unique pathways were further interrogated in both CJ+/Nl and CJ+/CJ- datasets, shown in Supplement Fig. S7, where plots of additional IPA transcript differences are apparent in both CJ+ comparisons. These transcripts further accentuate viral hypercytokinemia (not present in Arst/Nl vs Prol/Nl comparisons), stronger IFNα/β signaling, rheumatoid arthritis signaling, metalloproteinase activation, degradation of extracellular matrix and O-linked glycosylation that are not present in Arst/Nl samples. Thus during arrest, infected cells recruit an enhanced and more diverse immune response than that found in differentiating normal cells. Interestingly, several of these increases were not seen in CJ+ vs CJ- sample comparisons. This again underscores and expands the underlying changes in CJ- cells imprinted by prior infection that were brought out during re-arrest.

Arst/Nl cells, unlike CJ+ cells also displayed robust senescence pathway transcripts in addition to TP53 RNA signaling which regulates transcription of cell death genes. In this case senescence was linked to observed neurodifferentiation rather than cell death or degenerative changes. The widespread down regulation of proliferative elements in Nl cells, but not CJ+ cells, were also evaluated by Gene Enrichment Analysis shown in Supplement Fig. S8. Analysis of CJ+ vs Arst/Nl also revealed strong upregulation of α and γIFN targets. It also increased methylation, the opposite of the downregulated methylation in Nl cells. Methylation is a major regulator of stable epigenetic changes and methylation of cell cycle checkpoints may be one of the mechanisms that

permanently imprint the increased proliferative activity observed in CJ+ cells. CJ+ cells also show strong downregulation of clathrin endocytosis pathways and Cavin4 synaptic vesicle formation, both of which are reported to be central for PrP processing [34, 35]. Neither of these downregulated genes affected the steep rise in infectivity, The more central and major player TSE infection, Prnp was also downregulated 4 fold in CJ+ cells versus ArstNl cells. This RNA-seq data corresponds well with the more specific 5 fold RT/qPCR transcript downregulations previously. Moreover, corresponding PrP and PrP amyloid reductions of 3-5 fold by western blot were also documented different in passage assays [4]. PrP naïve infection. This is notable because there was no decrease in PrP by Western blots was not seen in SEP cells that had not be arrested previously. Downregulated Prnp in CJ+ samples is only one of 341 unique CJ+ changes by Venn diagram, along with a complete list of unique CJ+ transcripts in Supplement Fig. S9.

Unique CJ+ vs Arst/Nl show both upregulated (n=195) and downregulated (n=146) transcripts. This more complete data further supports many of the consolidated limited observations depicted above. However, additional transcripts, such as a few upregulated tumor suppressors and neural differentiation genes, that were not picked up by directed queries in IPA analyses, possibly because they have not been linked in the database to either neuronal differentiation or inflammation. These signify a complexity of network changes in SEP cells that may be useful for the discovery of other unifying features not addressed by the current analyses. This more detailed Supplement file S10 also shows the extensive fundamental difference in CJ+ versus other groups and the limited response of CJ- versus Nl cells indicates even more profound changes induced by prior and/or latent infection. There are only 40 upregulated unique changes induced in arrested CJ- cells (pink column) while there are 86 unique changes in the Nl comparison (light green). Downregulated genes show the same pattern, with only 18 differences in CJ- versus 26 in Nl comparisons. In sum, cDNA libraries demonstrated a multitude of previously unrecognized innate immune and anti-viral pathways activated by physiological arrest. Uninfected cells displayed a robust recruitment of neural

differentiation transcripts induced during perpetual arrest, along with a surprisingly wide variety of IFN and innate immune pathway responses. These pathways and transcripts were reproducible in independent experiments and appear to be integral to progressive differentiation and not due to underlying cytotoxic or added inflammatory stimuli. Arrest induced changes in latently infected CJ- cells showed marked differences from arrested uninfected control cells in proliferation, neuron differentiation and extent of innate immune responses. Since these CJ+ changes were not induced by arrest of uninfected cells, they are ultimately caused by infection. Of the many different transcript changes uncovered here, the most dramatic and far-reaching change was the release from proliferation controls. These underlie the partial escape from arrest as compared with the completely arrest of uninfected cells. At the same time CJ+ cells suppressed the neuron differentiation program of normal cells. These CJ+ differences strongly suggested a divergent phenotype imprinted by prior infection as discussed below.

DISCUSSION

Library cDNA construction with bioinformatics analysis uncovered previously unsuspected actors and global changes that could not be revealed by limited individual RT/qPCR studies. The data here expands the range of centrally involved pathways for proliferative control, neural differentiation, and IFN stimulated and other innate immune transcripts. In normal uninfected cells, conditional physiological arrest induced a total of 379 differentially expressed genes, and the overwhelming majority of the 204 downregulated transcripts suppressed DNA replication. Many upregulated anti-proliferative transcripts further targeted a diverse set of cell cycle checkpoint and mitotic cell transition controls, e.g. by inhibiting G1/S phase and mitotic transitions. These proliferative inhibitory changes were remarkably diverse and virtually complete by 6-7 days and were total by 14 days post arrest in all 3 independent experimental samples collected at 3 different times.

Arrest of normal cells also upregulated known neuron differentiation transcripts. Ingenuity pathway analysis highlighted 4 strong neuronal transcripts (AGTR2, NRG1, GDF6 and SFRP4) in

addition to 11 other neurodifferentiation transcripts including neuregulin, Prnp and HES6. HES6, a helix-loop-helix transcription repressor protein, that is mainly transcribed in brain and endocrine tissues, and this transcript may participate in epigenetic modifications of proliferation and neurodifferentiation features of SEP post-mitotic neurons. Arrest also downregulated methylation, a possible mechanism for epigenetic activation of selected neuronal transcripts. The basic cell fate of SEP cells was already imprinted when they were engineered to proliferate, and stable neural differentiation was documented post arrest. In cultured post-mitotic cerebrum neurons, stable differentiation and stimulus induced changes evaluated over several days revealed selective intron retention in the nucleus linked to these changes [36, 37]. Stable nuclear intron change may be informative for the widespread epigenetic anti-proliferative and innate immune features brought out by arrest of Nl cells. It may also operate in CJ agent induced epigenetic imprinting of latently infected peripheral white blood and/or lymphoid cells long before brain becomes infected.

Latently infected proliferating CJ- SEP cells with undetectable infectivity, that had been switched from a high infectivity CJ+ arrested state to a proliferating latent state for weeks, could not be distinguished from uninfected Nl proliferating cells by their behavior or morphology. Remarkably, these CJ- cells continued to differentially express several key differential transcripts versus proliferating Nl cells. This indicated that previous and/or inapparent latent infection was sufficient to change and permanently imprint a CJ altered phenotype as compared to uninfected Nl cells. These unique CJ- transcripts included upregulated acute phase protein LPB, C1s and Mt1M, an anti-inflammatory molecule [38] along with downregulated Cavin4 and neurodevelopment genes Tenm3 and Dpys13.

A variety of abundant altered proclivities of CJ- cells were brought out by re-arrest. The data here were reproducible in independent culture passages of cells re-arrested at different times up to 34 days. In contrast to Nl cells, high titer arrested CJ+ cells suppressed many Nl proliferative controls and enhanced innate immune cytokine/chemokine and inflammatory transcripts. For many years TSE

agents have been considered immunologically silent, largely because they elicit no typical lymphocytic infiltrates that are characteristic of acute and subacute viral infections, and no neutralizing antibodies have been found. The innate immune pathways in CJ+ were enriched compared to Nl arrested cells. Indeed, the CJ+ ratio of immune to proliferative changes was the reverse of arrested Nl transcripts, with innate immune pathways more upregulated while the proliferative pathways were downregulated with high infection (see Fig. 6). CJ+ cells also enhanced immune transcripts during the same time that the neuronal differentiation program was suppressed. This indicated that the enhancement of innate immune transcripts in CJ+ was not dependent on neuron differentiation. Previous direct RT/qPCR studies of β–IFN were also validated and expanded in CJ+ cells to include upregulation of many IFNα and IFNγ targets and cytokines. In acute viral infections, such as with Semliki virus, the response of immature neurons is augmented by β–IFN which reduces acute viral replication [39]. In contrast, multiple anti-viral transcripts and IFNs here failed to stop rapid CJ agent replication in SEP neurons. We are unaware of any form of recombinant host PrP or PrP amyloid that upregulates the IFNs or antiviral transcripts identified here. The molecular mechanism(s) inciting the enhanced CJ+ anti-viral and IFN activated transcripts observed here may be, at least in part, directly caused by the infectious ~20nm particle [6, 40], or indirectly signaled, as by agent induced dsRNA.

The 4-fold reduction of Prnp transcripts in CJ+ cells also correlated well with previous RT/qPCR and PrP protein studies [4]. A reduction in Prnp and PrP may even be part of a host defense mechanism imprinted by previous infection. Importantly, unlike re-arrested SEP cells, naïve SEP cells that were infected previously did not show a reduction in PrP. Instead these arrested CJ+ cells attained the same 8-10 fold increases of PrP as their Nl counterparts [5]. This comparison again strongly supports a retained epigenetic imprint in previously infected CJ- cells that reduced this essential susceptibility gene. This reduction in Prnp failed to limit high levels of infection. Downregulated Cavin4, a caveolar protein in lipid rafts thought to be required for conversion of non-

pathogenic PrP to the infectious scrapie amyloid form [35], also failed to suppress high levels of infection. Other transcripts, possibly some metalloproteinases found here, may be more essential in this host amyloid conversion that does not replicate like the infectious agent.

Although neurons were originally thought to be the only cells with high infectivity, possibly because they show high levels of PrP amyloid, CJ brain infection activated myeloid microglia These activated microglia were purified, and they contained barely detectable PrP and no detectable PrP amyloid. Nonetheless, they carried maximal brain titers [41]. Notably, these highly infectious microglia also displayed several IFN activated and regulated genes, e.g., IFI204, IRF2 and IRF8, and several other immune and inflammatory responses appeared after stimulation by poly I:C (e.g., ISG15, CXCL10 and OAS) [42]. Those genes corresponded to CJ+ SEP transcripts identified here. Moreover, in CJD infected mouse brains, the IFN linked transcripts IFI204, IFI 202, CXCL10 and IFR8 were elevated during initial early infection at 10-40 days post-inoculation, when agent doubling begins, a period well before PrP amyloid and clinical signs became detectable. This critical early period of infection is rarely studied. Subsequent brain studies revealed the cytokines TGFα, IL1β, and MIP-1α and β chemokines were also elevated ≥10-fold by 30 days post FU-CJD intracerebral inoculation [43]. Since none of these changes were present in mice inoculated with uninfected brain, they represent an important recognition by the host of the infectious agent. In rats, activated microglia appear midway in the incubation with spongiform changes and it takes 100 days more for PrP amyloid to become detectable [8]. This further substantiates host innate immune responses to the CJ agent that are unrelated to PrP amyloid. RNA-seq potentially can reveal additional shared pathways among CJ+ microglia, CJ+ SEP neurons and CJ+ dendritic gut cells that do exhibit diagnostic PrP amyloid early after peripheral infection [44]. Although some specific molecules recruited by high infection may vary in different cell types and species, their comparable functions and overlapping pathways appear to be generalized.

While little is known about latency in peripheral cells that are first infected via natural routes of infection, e.g., via skin abrasion (endemic scrapie) and oral (epidemic BSE) routes,TSE experimental studies clearly show myeloid cells and lymphoid harbor infection for extended times, especially with low dose infections that may not be manifest during an animal's normal lifespan. Unlike cell cultures, animals have many additional cellular and humoral ways to hide and restrict TSE agent replication as evidenced by rapid TSE agent replication after transfer from mice to murine cell cultures. A variety of TSE agents consistently double every 19-24 hours in GT1 neuron derived cultures but have dramatically longer clearly strain-specific 5-25 day doubling times in mice inoculated intracerebrally [20, 45]. A variety of cells and many different host responses, including common lysosomal clearance mechanisms, and PrP amyloid itself, can retard or even eliminate infection [9]. But the specific TSE agent inhibitors in vivo remain uncharted, especially in peripheral lymphoid tissue where these agents silently persist for many years. In the current SEP experiments CJ agent replication was remarkably rapid in arrested cells and achieved very high titers within 34 days without obvious toxic effects. It is apparent that these cells were primed to activate and replicate agent even before PrP had reached its peak production [4],

The most profound and global change uncovered by RNA-seq was that re-arrested CJ+ cells subverted a plethora of proliferative controls. These led to a permanent partial escape from physiological arrest reflected in the growth of these cells. These changes are part of the fundamental biology of TSE infection in both scrapie and CJD including non-neuronal cell types. Although largely forgotten, faster growth of explanted scrapie and CJD infected brain cells are reproducible. Faster growth rates were independently reported by 4 different laboratories [46]. They include rapidly proliferating permanent agent-producing cell lines in addition to those that lost infectivity. Some of these cell lines show a transformed immortal phenotype with loss of contact inhibition, and others formed huge tumors on heterologous transplantation to nude mice. These included sCJD human brain

cultures and sCJD infected hamster cells [47]. This transformation feature, in addition to latency, is characteristic of DNA viruses.

Although there is widespread belief that misfolded host PrP amyloid is infectious without any nucleic acid [48], infection by recombinant PrP amyloid ("the gold standard of proof") has not been reproducible, and synthetic recombinant PrP aggregates are pathological when inoculated in brain, but not infectious, e.g., [49-51]. While there is no definitive TSE-specific sequence for the virus-like ~20nm particle observed in highly infectious cell fractions and in infected cells, TSE brain and culture particle fractions contain circular DNAs of 1-3kb with phage linked REP sequences that have also been identified in human non-TSE samples elsewhere [52-54]. While not specific for TSEs, other circular DNAs in infectious fractions may be more TSE specific. In any case, a nucleic acid component of the infectious particle can't be excluded, especially because nucleases destroy 3 logs of infectivity in CJD and scrapie fractions while PrP-amyloid is preserved [55]. Given the presence of DNA in all highly infectious fractions examined with modern molecular amplification techniques and sequencing, the strong proliferative and latent infection changes shown here and the known stability of TSE agent-strains, a DNA element that can define individual agent strains is worth considering.

We examined only a single human TSE agent strain here, and other agents such as sheep derived scrapie, BSE, and cervid agents may not show to the same pattern of responses even though the fundamental modes of agent spread, latency, and basic brain pathology are common to all TSE strains. Arrest caused far more complex and abundant changes in CJ+ compared to uninfected Nl cells than to CJ- cells, and this along with other data here showed CJ- cells were primed to respond differently than Nl SEP cells, i.e., they retained a cellular memory of their past and latent infection. Although the mechanism(s) of imprinting is not clear, upregulated methylation of CJ selected genes in SEP neurons could perpetuate episomal modifications of at lease some proliferative escape transcripts. Additionally, human sCJD, and sCJD infected mouse brains that analyzed all cell types showed "epitranscriptomic" profile changes with altered RNA edited pathways in later stages of disease

[56]. Such profile changes along with retained nuclear introns [37] mechanistically might also apply here. In any case, cells latently infected at undetectable or even moderate levels, as in animal spleen and lymphoid myeloid cells, may be manipulated by culture conditions, or stressed to uncover hidden diagnostic and infection driven changes such as increased proliferation and/or unique innate immune transcript patterns. These could be rapidly assayed by RT/qPCR.

In conclusion, the current results bring to the fore many common biologic, virologic and episomally altered activation pathways that may be exploited for diagnosis of latently infected cells, such as myeloid blood cells that disseminate TSE agents to the brain [14], and in selected tissue myeloid derived dendritic cells [44, 57] that can be latently infected years before they become productively infectious.

REFERENCES

1. Cajal, S.R., *Histologie du Systeme Nerveux de L'homme & des vetebres*. Vol. II. 1955, Madrid Spain Instituto Ramon y Cajal.
2. Eves, E., et al., *Conditional immortalization of neuronal cells from postmitotic cultures and adult CNS.* Brain Res., 1994. **656**: p. 396-404.
3. Miyazawa, K., K. Emmerling, and L. Manuelidis, *Proliferative arrest of neural cells induces prion protein synthesis, nanotube formation, and cell-to-cell contacts.* J Cell Biochem, 2010. **111**(1): p. 239-47.
4. Aguilar, G., N. Pagano, and L. Manuelidis, *Reduced Expression of Prion Protein With Increased Interferon-beta Fail to Limit Creutzfeldt-Jakob Disease Agent Replication in Differentiating Neuronal Cells.* Front Physiol, 2022. **13**.
5. Miyazawa, K., et al., *Continuous production of prions after infectious particles are eliminated: implications for Alzheimer's disease.* PLoS One, 2012. **7**(4): p. e35471.
6. Manuelidis, L., et al., *Cells infected with scrapie and Creutzfeldt-Jakob disease agents produce intracellular 25-nm virus-like particles.* Proc Natl Acad Sci U S A, 2007. **104**(6): p. 1965-70.
7. Büeler, H., et al., *Mice devoid of PrP are resistant to scrapie.* Cell, 1993. **73**: p. 1339-1347.
8. Manuelidis, L., W. Fritch, and Y.G. Xi, *Evolution of a strain of CJD that induces BSE-like plaques.* Science, 1997. **277**: p. 94-98.
9. Manuelidis, L., *Infectious particles, stress, and induced prion amyloids: a unifying perspective.* Virulence, 2013. **4**(5): p. 373-83.
10. Gajdusek, D.C., *Unconventional viruses and the origin and disappearance of kuru.* Science, 1977. **197**: p. 943-960.
11. Manuelidis, E. and L. Manuelidis, *Clinical and Morphologic Aspects of Transmissible Creutzfeldt-Jakob Disease*, in *Progress in Neuropathology*, H.M. Zimmerman, Editor. 1979, Raven Press: N.Y. p. 1-26.
12. Wilson, D.R., R.D. Anderson, and W. Smith, *Studies in scrapie.* J Comp Pathol, 1950. **60**(4): p. 267-82.
13. Eklund, C.M., R.C. Kennedy, and W.J. Hadlow, *Pathogenesis of scrapie virus infection in the mouse.* J Infect Dis, 1967. **117**(1): p. 15-22.

14. Manuelidis, E.E., E.J. Gorgacs, and L. Manuelidis, *Viremia in experimental Creutzfeldt-Jakob disease.* Science, 1978. **200**(4345): p. 1069-71.
15. Fraser, H.a.D., AG, *Scrapie in mice. Agent strain diffeences in the distribution and intensity of grey matter vacuolization.* J Comp Pathol, 1973. **83**: p. 29-40.
16. Manuelidis, L., *Vaccination with an attenuated CJD strain prevents expression of a virulent agent.* Proc. Natl. Acad. Sci. USA, 1998. **95**: p. 2520-2525.
17. Arjona, A., et al., *Two Creutzfeldt-Jakob disease agents reproduce prion protein-independent identities in cell cultures.* Proc Natl Acad Sci USA, 2004. **101**: p. 8768-8773.
18. Manuelidis, L. and Z.Y. Lu, *Virus-like interference in the latency and prevention of Creutzfeldt-Jakob disease.* Proc. Natl. Acad. Sci. USA, 2003. **100**: p. 5360-5365.
19. Nishida, N., S. Katamine, and L. Manuelidis, *Reciprocal interference between specific CJD and scrapie agents in neural cell cultures.* Science, 2005. **310**(5747): p. 493-6.
20. Manuelidis, L., et al., *The kuru infectious agent is a unique geographic isolate distinct from Creutzfeldt-Jakob disease and scrapie agents.* Proc Natl Acad Sci U S A, 2009. **106**(32): p. 13529-34.
21. Liu, Y., et al., *A rapid accurate culture assay for infectivity in Transmissible Encephalopathies.* J Neurovirol, 2008. **14**(5): p. 352-61.
22. Dobin, A., et al., *STAR: ultrafast universal RNA-seq aligner.* Bioinformatics, 2013. **29**(1): p. 15-21.
23. Love, M.I., W. Huber, and S. Anders, *Moderated estimation of fold change and dispersion for RNA-seq data with DESeq2.* Genome Biol, 2014. **15**(12): p. 550.
24. Benjamini, Y. and Y. Hochberg, *Controlling the false discovery rate: a practical and powerful approach to multiple testing.* Journal of the Royal statistical society: series B (Methodological), 1995. **57**(1): p. 289-300.
25. Subramanian, A., et al., *Gene set enrichment analysis: a knowledge-based approach for interpreting genome-wide expression profiles.* Proc Natl Acad Sci U S A, 2005. **102**(43): p. 15545-50.
26. Kolberg, K., et al., *g:Profiler—interoperable web service for functional enrichment analysis and gene identifier mapping (2023 update).* Nucleic Acids Research.
27. Shannon, P., et al., *Cytoscape: a software environment for integrated models of biomolecular interaction networks.* Genome Res, 2003. **13**(11): p. 2498-504.
28. Manuelidis, E., et al., *Serial propagation of Creutzfeldt-Jakob disease in guinea pigs.* Proc. Natl. Acad. Sci. (USA), 1976. **73**: p. 223-227.
29. New, C., et al., *Tetraspanins: Host Factors in Viral Infections.* Int J Mol Sci, 2021. **22**(21).
30. Samuelov, L., et al., *SVEP1 plays a crucial role in epidermal differentiation.* Exp Dermatol, 2017. **26**(5): p. 423-430.
31. Jhas, S., et al., *Hes6 inhibits astrocyte differentiation and promotes neurogenesis through different mechanisms.* J Neurosci, 2006. **26**(43): p. 11061-71.
32. Das Gupta, S., et al., *Dynamics of clusterin protein expression in the brain and plasma following experimental traumatic brain injury.* Sci Rep, 2019. **9**(1): p. 20208.
33. Thomas, A., et al., *Expression of a complete and functional complement system by human neuronal cells in vitro.* Int Immunol, 2000. **12**(7): p. 1015-23.
34. Shyng, S.L., J.E. Heuser, and D.A. Harris, *A glycolipid-anchored prion protein is endocytosed via clathrin-coated pits.* J Cell Biol, 1994. **125**(6): p. 1239-50.
35. Vey, M., et al., *Subcellular colocalization of the cellular and scrapie prion proteins in caveolae-like membranous domains.* Proc Natl Acad Sci U S A, 1996. **93**(25): p. 14945-9.
36. Yeom, K.H., et al., *Tracking pre-mRNA maturation across subcellular compartments identifies developmental gene regulation through intron retention and nuclear anchoring.* Genome Res, 2021. **31**(6): p. 1106-1119.
37. Mazille, M., et al., *Stimulus-specific remodeling of the neuronal transcriptome through nuclear intron-retaining transcripts.* EMBO J, 2022. **41**(21): p. e110192.
38. Dai, H., et al., *Metallothionein 1: A New Spotlight on Inflammatory Diseases.* Front Immunol, 2021. **12**: p. 739918.
39. Narayanan, D., et al., *Immature Brain Cortical Neurons Have Low Transcriptional Competence to Activate Antiviral Defences and Control RNA Virus Infections.* J Innate Immun, 2023. **15**(1): p. 50-66.
40. Manuelidis, L., *A 25 nm virion is the likely cause of transmissible spongiform encephalopathies.* J Cell Biochem, 2007. **100**(4): p. 897-915.

41. Baker, C.A., D. Martin, and L. Manuelidis, *Microglia from Creutzfeldt-Jakob disease-infected brains are infectious and show specific mRNA activation profiles.* J Virol, 2002. **76**(21): p. 10905-13.
42. Baker, C.A., Z.Y. Lu, and L. Manuelidis, *Early induction of interferon-responsive mRNAs in Creutzfeldt-Jakob disease.* J Neurovirol, 2004. **10**(1): p. 29-40.
43. Lu, Z.H., C. Baker, and L. Manuelidis, *New molecular markers of early and progressive CJD brain infection.* J. Cellular Biochem., 2004. **93**: p. 644-652.
44. Shlomchik, M.J., et al., *Neuroinvasion by a Creutzfeldt-Jakob disease agent in the absence of B cells and follicular dendritic cells.* Proc Natl Acad Sci U S A, 2001. **98**(16): p. 9289-94.
45. Miyazawa, K., K. Emmerling, and L. Manuelidis, *Replication and spread of CJD, kuru and scrapie agents in vivo and in cell culture.* Virulence, 2011. **2**(3): p. 188-99.
46. Manuelidis, E., et al., *Immortality of cell cultures derived from brains of mice and hamsters infected with Creutzfeldt-Jakob disease agent.* Proc. Natl. Acad. Sci., 1987. **84**: p. 871-875.
47. Manuelidis, E., Kim, JH, Manuelidis, L, *Novel biologic properties of Creutzfeldt-Jacob infected brains in vitro*. Biologic aspects of Alzheimer's Disease, ed. R. Katzman. Vol. Banbury Report 1983, Cold Spring Harbor, NY: Cold Spring Harbor Laboratory.
48. Prusiner, S., *The Nobel Lecture: Prions.* Proc Natl Acad Sci U S A., 1998. **95**(23): p. 13363–13383.
49. Timmes, A.G., et al., *Recombinant prion protein refolded with lipid and RNA has the biochemical hallmarks of a prion but lacks in vivo infectivity.* PLoS One, 2013. **8**(7): p. e71081.
50. Barron, R.M., et al., *PrP aggregation can be seeded by pre-formed recombinant PrP amyloid fibrils without the replication of infectious prions.* Acta Neuropathologica, 2016. **132**(4): p. 611-624.
51. Schmidt, C., et al., *A systematic investigation of production of synthetic prions from recombinant prion protein.* Open Biol, 2015. **5**(12): p. 150165.
52. Manuelidis, L., *Nuclease resistant circular DNAs copurify with infectivity in scrapie and CJD.* J Neurovirol, 2011. **17**(2): p. 131-45.
53. Yeh, Y.H., V. Gunasekharan, and L. Manuelidis, *A prokaryotic viral sequence is expressed and conserved in mammalian brain.* Proc Natl Acad Sci U S A, 2017. **114**(27): p. 7118-7123.
54. Zur Hausen, H., T. Bund, and E.M. de Villiers, *Infectious Agents in Bovine Red Meat and Milk and Their Potential Role in Cancer and Other Chronic Diseases.* Curr Top Microbiol Immunol, 2017.
55. Botsios, S. and L. Manuelidis, *CJD and Scrapie Require Agent-Associated Nucleic Acids for Infection.* J Cell Biochem, 2016. **117**(8): p. 1947-58.
56. Kanata, E., et al., *RNA editing alterations define manifestation of prion diseases.* Proc Natl Acad Sci U S A, 2019. **116**(39): p. 19727-19735.
57. Radebold, K., et al., *Blood borne transit of CJD from brain to gut at early stages of infection.* BMC Infect Dis. 2001; 1: 20., 2001: p. 1-5.

Acknowledgments: We are indebted to Brett Robb and NEB for making the ribosomal-deleted RNA-seq libraries. This work was supported by the Hanna Howard Fund, a gift from the William Prusoff Foundation to LM and in part by NINDS/NIH Award R01NS122907. Access to Partek Flow (Illumina), Qlucore Omics Explorer (Qlucore), and Ingenuity Pathway Analysis (Qiagen) was provided and sponsored by the Cushing/Whitney Medical Library, Yale School of Medicine.

Figures and Tables

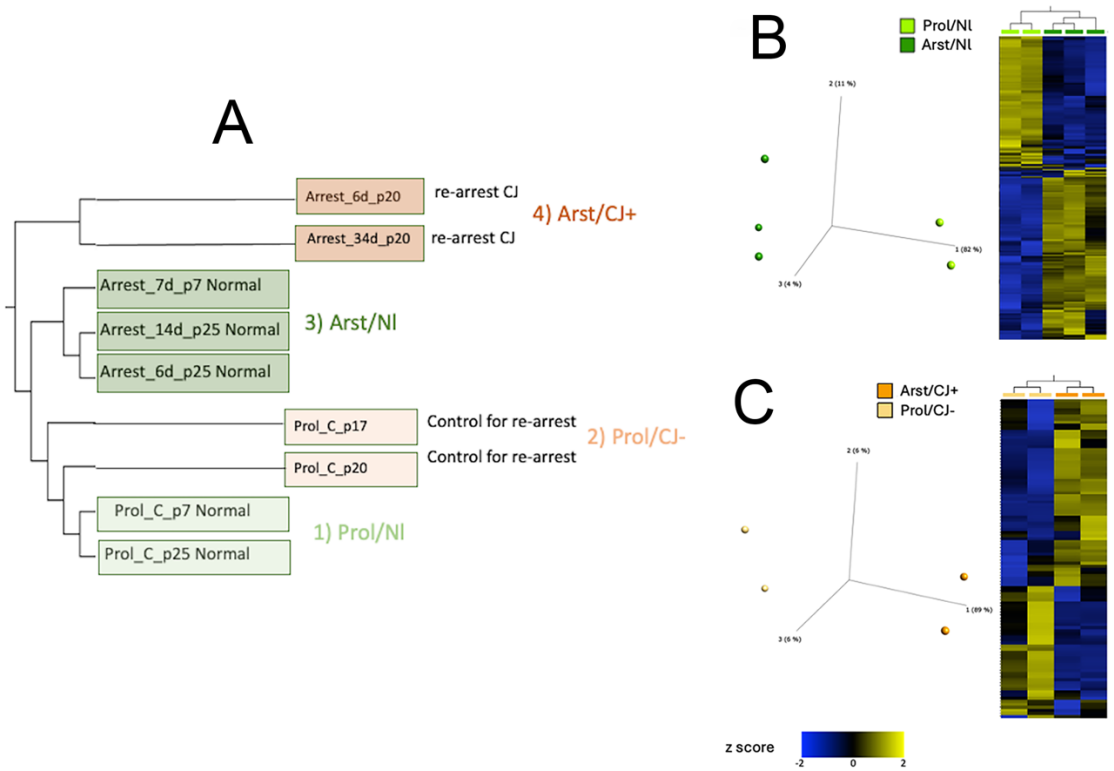

Fig. 1. A): Hierarchical clustering of different passages (p) and days based on 22,251 normalized genes. Proliferating Nl controls (light green, p7 & p25) were closely related to Proliferating CJ- cells (light red, p17 & p20). Arrested Nl cells in darker green and red (CJ) area were also more closely related to arrested CJD infected cells (groups 3 & 4 respectively) than to their proliferating counterparts. **B**): Principal component analysis (PCA) and hierarchical clustering heatmap comparing Nl proliferating and Nl arrested cell sets. DESeq2 differential analysis (FDR $p<0.05$, Fold change>|2|) resulted in 379 differentially expressed genes between these 2 groups (205 downregulated and 174 upregulated). **C**) Principal component analysis (PCA) and hierarchical clustering heatmap comparing CJ- proliferating and CJ+ arrested cell sets yielding a total of 112 genes. DESeq2 differential analysis (FDR $p<0.05$, Fold change>|2|) resulted in differentially expressed genes between these 2 groups (45 downregulated and 67 upregulated).

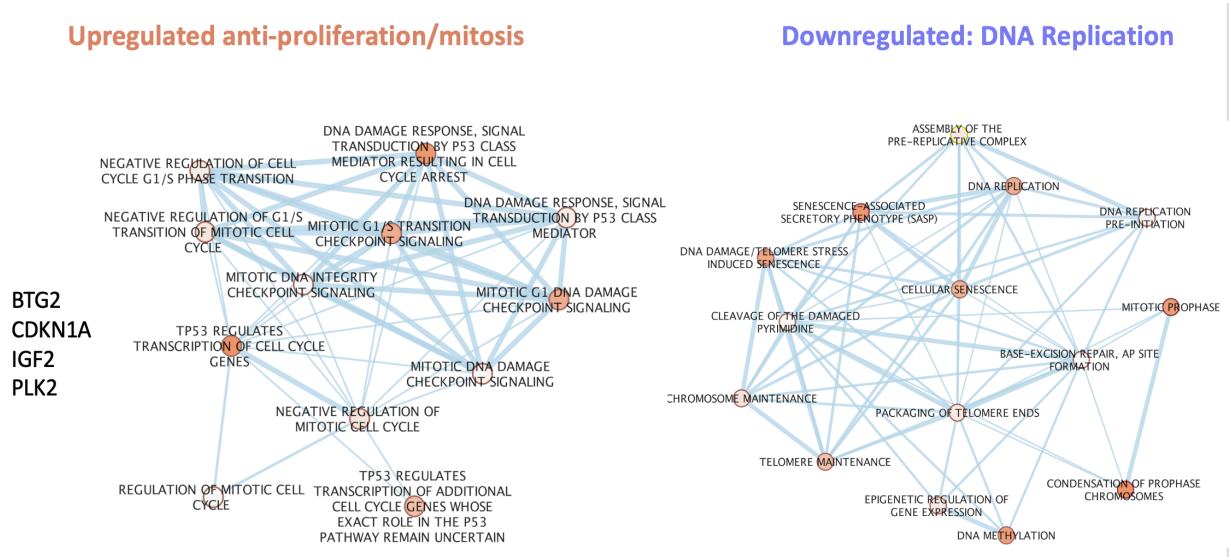

Fig. 2. Overrepresentation analysis and clustering analysis of enriched pathways with upregulated and downregulated genes contributing to arrest of the p7 day 7. g:Profiler web server was used for overrepresentation analysis. Enriched signatures was analyzed with Enrichment map application and was visualized on Cytoscape

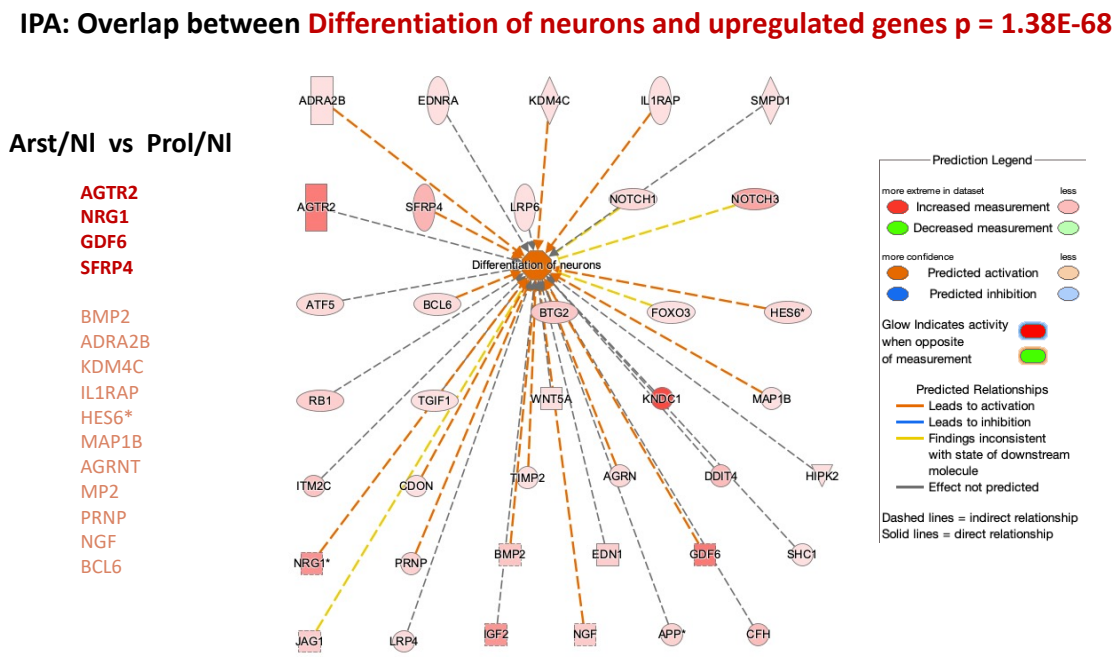

Fig. 3 Ingenuity pathway analysis shows significant overlap (p=1.38E-68) between neural differentiation and upregulated differentially expressed transcripts in Arst/Nl samples. Differentiation of neuronal function is predicted to be activated (dark orange color). Higher expressed genes are genes shown in darker red color.

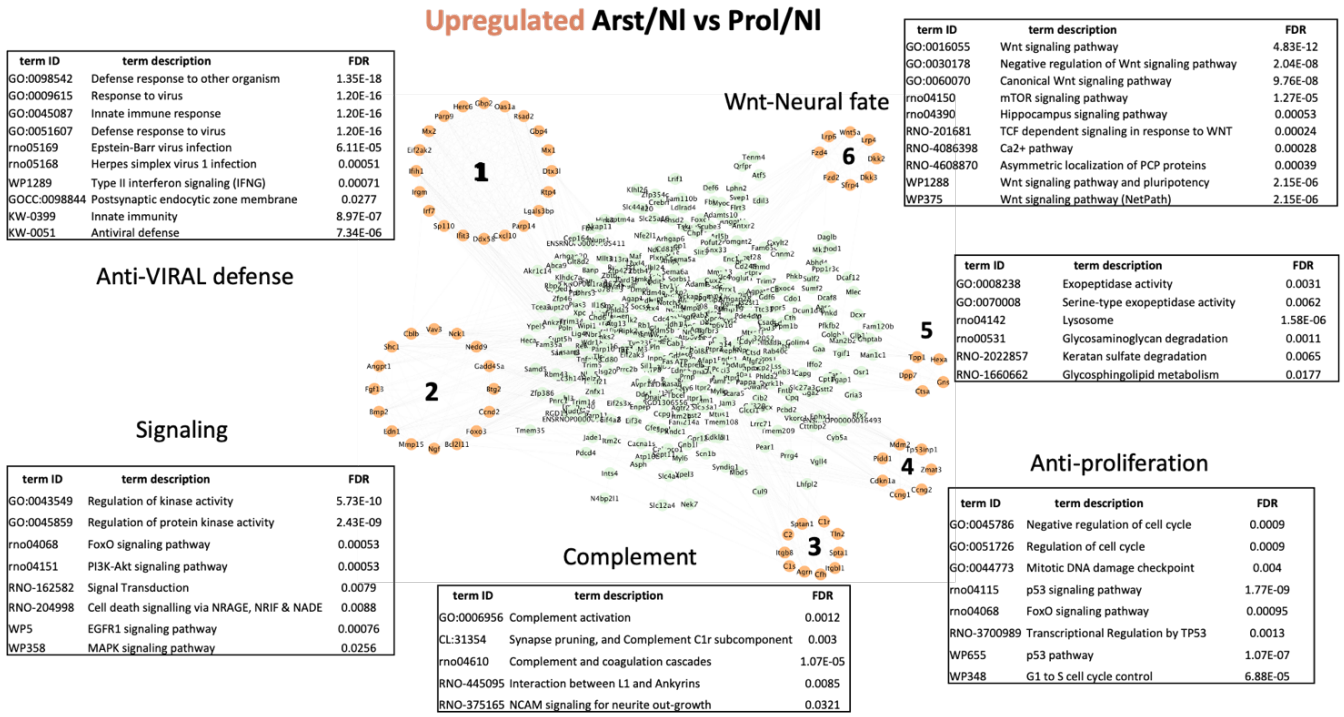

term ID	term description	FDR
GO:0098542	Defense response to other organism	1.35E-18
GO:0009615	Response to virus	1.20E-16
GO:0045087	Innate immune response	1.20E-16
GO:0051607	Defense response to virus	1.20E-16
rno05169	Epstein-Barr virus infection	6.11E-05
rno05168	Herpes simplex virus 1 infection	0.00051
WP1289	Type II interferon signaling (IFNG)	0.00071
GOCC:0098844	Postsynaptic endocytic zone membrane	0.0277
KW-0399	Innate immunity	8.97E-07
KW-0051	Antiviral defense	7.34E-06

term ID	term description	FDR
GO:0016055	Wnt signaling pathway	4.83E-12
GO:0030178	Negative regulation of Wnt signaling pathway	2.04E-08
GO:0060070	Canonical Wnt signaling pathway	9.76E-08
rno04150	mTOR signaling pathway	1.27E-05
rno04390	Hippocampus signaling pathway	0.00053
RNO-201681	TCF dependent signaling in response to WNT	0.00024
RNO-4086398	Ca2+ pathway	0.00028
RNO-4608870	Asymmetric localization of PCP proteins	0.00039
WP1288	Wnt signaling pathway and pluripotency	2.15E-06
WP375	Wnt signaling pathway (NetPath)	2.15E-06

term ID	term description	FDR
GO:0008238	Exopeptidase activity	0.0031
GO:0070008	Serine-type exopeptidase activity	0.0062
rno04142	Lysosome	1.58E-06
rno00531	Glycosaminoglycan degradation	0.0011
RNO-2022857	Keratan sulfate degradation	0.0065
RNO-1660662	Glycosphingolipid metabolism	0.0177

term ID	term description	FDR
GO:0043549	Regulation of kinase activity	5.73E-10
GO:0045859	Regulation of protein kinase activity	2.43E-09
rno04068	FoxO signaling pathway	0.00053
rno04151	PI3K-Akt signaling pathway	0.00053
RNO-162582	Signal Transduction	0.0079
RNO-204998	Cell death signalling via NRAGE, NRIF & NADE	0.0088
WP5	EGFR1 signaling pathway	0.00076
WP358	MAPK signaling pathway	0.0256

term ID	term description	FDR
GO:0006956	Complement activation	0.0012
CL:31354	Synapse pruning, and Complement C1r subcomponent	0.003
rno04610	Complement and coagulation cascades	1.07E-05
RNO-445095	Interaction between L1 and Ankyrins	0.0085
RNO-375165	NCAM signaling for neurite out-growth	0.0321

term ID	term description	FDR
GO:0045786	Negative regulation of cell cycle	0.0009
GO:0051726	Regulation of cell cycle	0.0009
GO:0044773	Mitotic DNA damage checkpoint	0.004
rno04115	p53 signaling pathway	1.77E-09
rno04068	FoxO signaling pathway	0.00095
RNO-3700989	Transcriptional Regulation by TP53	0.0013
WP655	p53 pathway	1.07E-07
WP348	G1 to S cell cycle control	6.88E-05

Fig. 4: Interaction network analysis of upregulated differentially expressed genes in Arst/Nl vs Prol/Nl. Interaction network was built using STRING knowledgebase (v. 12.0). The resulting network was imported into Cytoscape (v. 3.10.2), and clustering analysis was performed with MCODE application (v. 2.0.3) using a degree cutoff 2, node density cutoff 0.1, K-core 2, and maximum depth 100. Resulting clusters were functionally annotated on STRING knowledgebase.

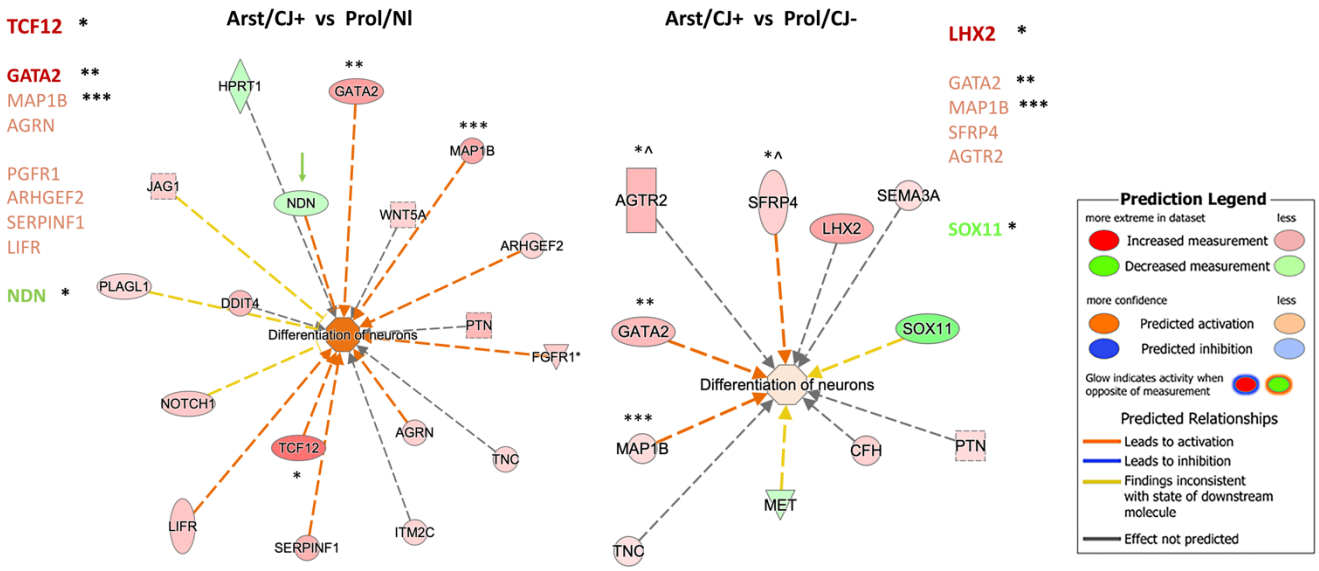

Fig. 5. A) Ingenuity pathway analysis shows significant overlap (and activation) between differentially expressed genes and neuron differentiation in Arst/CJ+ vs Prol/Nl arrested cells (A),but it is reduced as compared to stronger activation in Arst /Nl vs Prol/Nl transcripts (compare Fig. 3). The differentiation of neurons is even less activating in B) that shows Arst/CJ+ vs Prol/CJ- differences. Note the pale pink center in B with the darker red neuronal activation in A. The transcripts are also different in each of these CJ+ comparisons with only Map18 shared (***) in all 3 comparisons. GATA2 was activated only in these two CJ+ comparisons, but not in Arst/Nl cells (**) , and two stronger transcripts (TCF12 and LHX2) were found only in a single comparison (*). Strong NGR2, GDF6 & SFR4 signals seen in Arst/Nl samples (see Fig. 3) are absent in these CJ+ comparisons and strong Nl AGTR2 is absent or diminished in the CJ+ comparisons above.

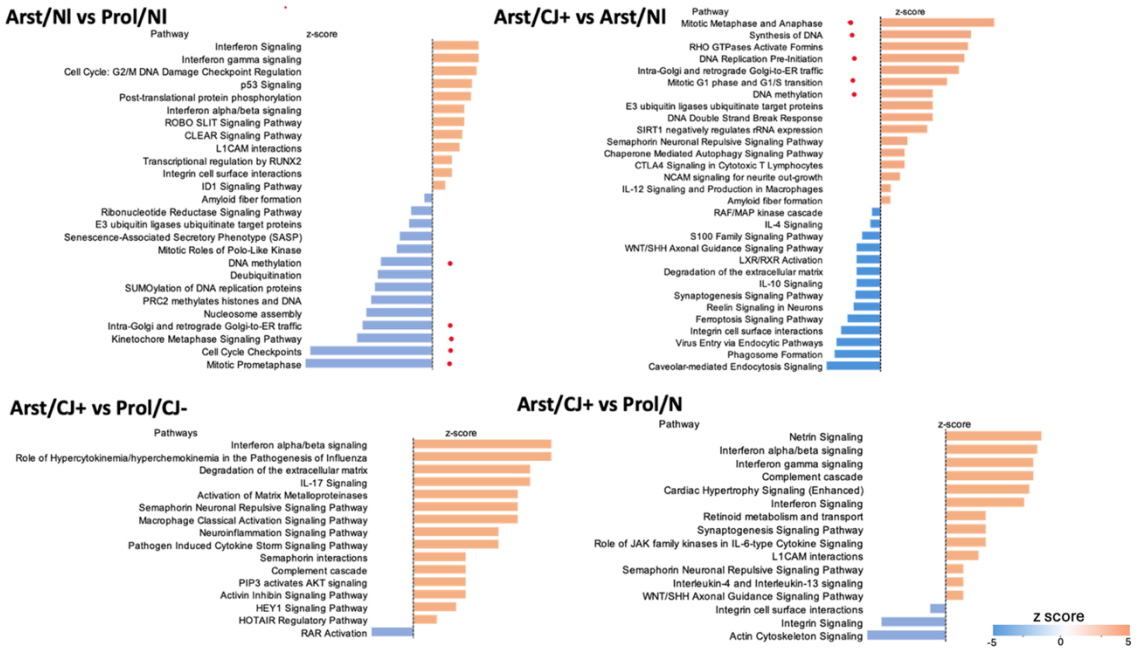

Fig 6. Ingenuity pathway analysis showing overrepresented pathways (Fisher's exact test FDRp<0.05), and activation status prediction based on z-score for the comparison of different sets of infected and uninfected cells. Positive z-score (orange bars) indicates pathway activation while negative z-score (blue bars) indicate inhibition.

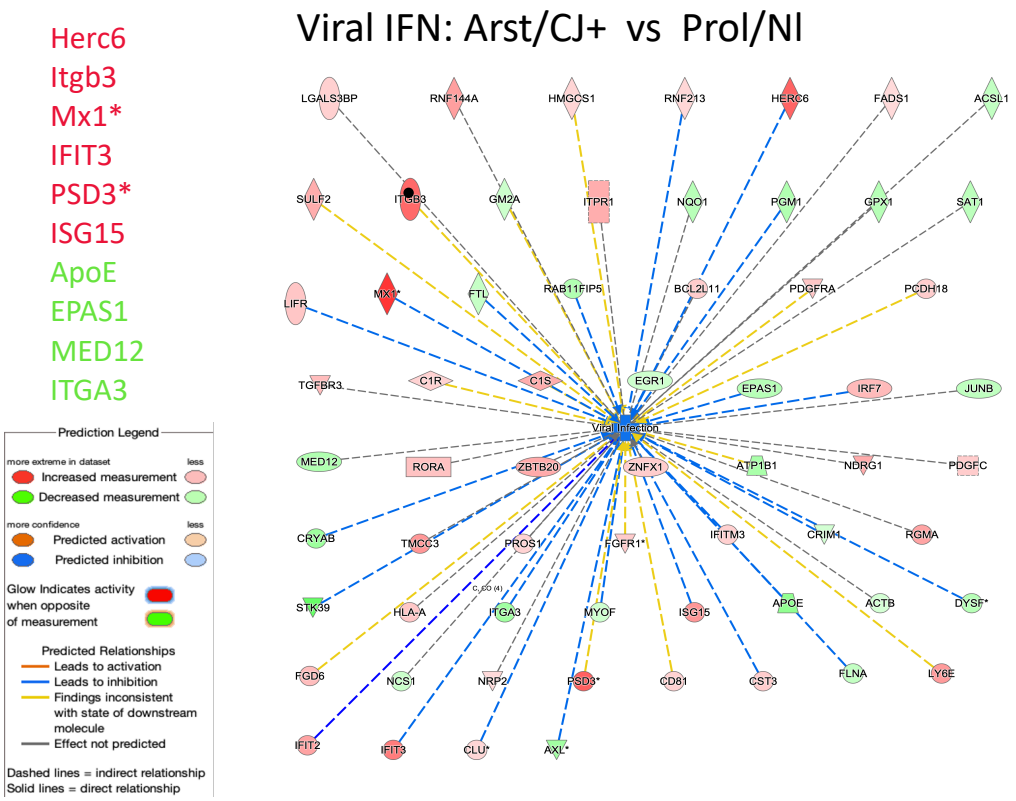

Fig. 7: Ingenuity pathway analysis overlap between differentially expressed genes and viral infection function. Strong anti-viral activation (blue lines) from transcripts up regulated in CJ+ cells. Mx1 gene protects against viruses that replicate in the nucleus, possibly indicative of a CJ+ DNA component. Although PSD3 (plectin) is captured here by ingenuity viral pathways (without a consistent role), it is highly expressed in neurons but was not IPA linked to neuronal function or differentiation (see Fig. 3).

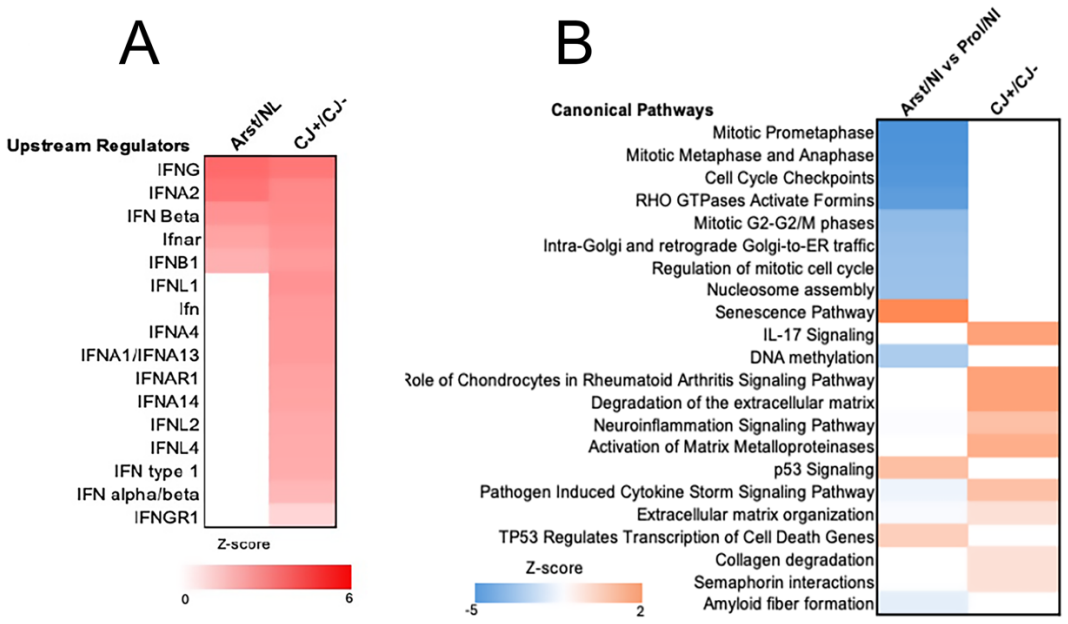

Fig. 8 Ingenuity pathway analysis of upstream regulators. Comparison of upstream regulators and examples of canonical pathways that differ in Arst/Nl and CJ+ cells. A) shows activation status (based on z-score) of expressed upstream IFN regulators (red) not present in Arst/Nl cells. B) shows canonical pathways. Note other signature transcripts upregulated (orange) in CJ+ and DNA methylation and cell cycle controls are downregulated (blue).